CHAPTER 16

THERMODYNAMIC PRINCIPLES OF SELF-ASSEMBLY

16.1 INTRODUCTION

In Part III we shall be looking at the interactions of small molecular aggregates such as micelles, bilayers, vesicles and biological membranes, which form readily in aqueous solution by the spontaneous *self-association* or *self-assembly* of certain amphiphilic molecules (see Figs 16.1 and 16.2 and Table 16.1). These structures and the systems they form—sometimes collectively referred to as *association colloids* or *complex fluids*—stand apart from the conventional colloidal particles discussed in Part II in one important respect: unlike solid particles or rigid macromolecules such as DNA, they are soft and flexible, i.e., *fluid-like*. This is because the forces that hold amphiphilic molecules together in micelles and bilayers are not due to strong covalent or ionic bonds but arise from weaker van der Waals, hydrophobic, hydrogen-bonding and screened electrostatic interactions. Thus, if the solution conditions, such as the electrolyte concentration or the pH, of an aqueous suspension of micelles or vesicles is changed, not only will this affect the interactions between the aggregates but it will also affect the intermolecular forces within each aggregate, thereby modifying the size and shape of the structures themselves. It is therefore necessary to begin by considering the factors that determine how and why certain molecules associate into various well-defined structures.

In Chapters 16 and 17 we shall be concerned with the thermodynamic and physical principles of self-assembly in general and of amphiphilic molecules such as surfactants and lipids in particular, while in the final Chapter 18 we shall investigate the various forces between amphiphilic structures and surfaces, and examine their role in the interactions of, for example, lipid vesicles and biological membranes.

Our first concern will be to formulate the basic equations of self-assembly in general statistical thermodynamic terms and then go on to investigate the relevant intermolecular interactions that determine into which structures

TABLE 16.1 Some common amphiphiles

Single-chained surfactants

Anionic	$C_{12}H_{25}—O\text{-}SO_3^-\,Na^+$	Sodium dodecyl sulphate (SDS or NaDS)
Anionic	$C_{18}H_{37}—COO^-\,H^+$	Stearic acid
Cationic	$C_{16}H_{33}—N^+(CH_3)_3Br^-$	Hexadecyl trimethylammonium bromide (HTAB or CTAB)
Non-ionic	$C_{12}H_{25}—(O\text{-}CH_2\text{-}CH_2)_5\text{-}OH$	Pentaoxyethylene dodecyl ether ($C_{12}E_5$)
Zwitterionic	Single chained lecithin (see below)	Lysolecithin

Double-chained phospholipids

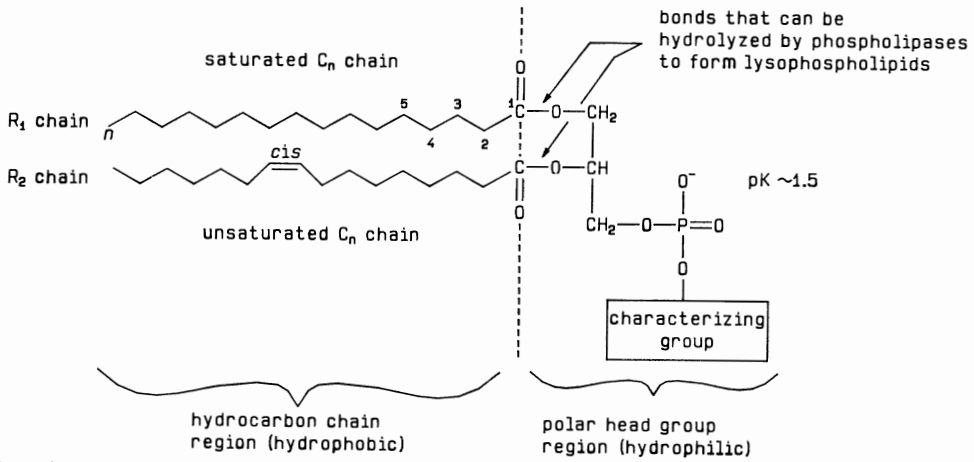

Hydrocarbon chains[a]	Name of phospholipid[b]	Characterizing group[c]
Normally contain 16–18 carbons per chain, the R_2 chain containing 1–3 *cis*	...phosphatidic acid (anionic)	—H pK ~ 11
diC_{12}: *dilauroyl*...	...phosphatidyl choline or lecithin (zwitterionic)	$—CH_2—CH_2—N^+(CH_3)_3$
diC_{14}: dimyristoyl...	...phosphatidyl ethanolamine (zwitterionic)	$—CH_2—CH_2—NH_3^+$ pK ~ 11
diC_{16}: dipalmitoyl...	...phosphatidyl glycerol (anionic)	$—CH_2—CH(CH_2OH)(OH)$
diC_{18}: distearoyl...	...phosphatidyl serine (anionic)	$—CH_2—CH(COO^-)(NH_3^+)$

Other double-chained surfactants and lipids[b]

Dihexadecyl dimethylammonium bromide ($diC_{16}DAB$)

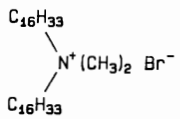

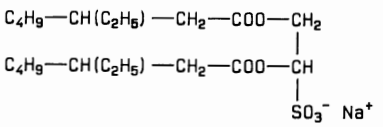

Aerosol OT

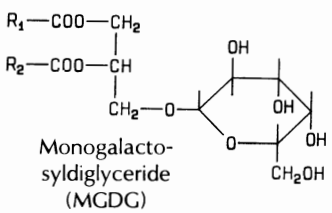

Monogalacto-syldiglyceride (MGDG)

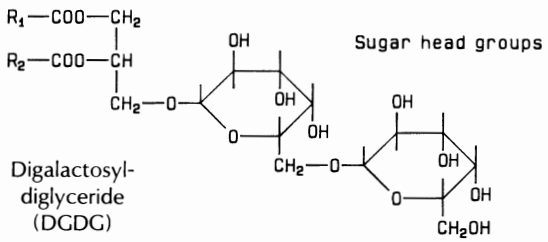

Sugar head groups

Digalactosyl-diglyceride (DGDG)

[a] About 50% of biological lipids have an unsaturated chain; these increase the fluidity and hydrophilicity of bilayers.

[b] Phosphatidylcholines and phosphatidylethanolamines are the two major lipids found in animal membranes, while the galactolipids DGDG and MGDG are the major constituents of plant thylakoid membranes. Note that none of these carry a net charge at normal pH.

[c] The ionic states of the headgroups are given for aqueous dispersions at pH 7. At high pH (> 11.5) phosphatidylethanolamine becomes negatively charged while at low pH (< 1) it becomes positively charged.

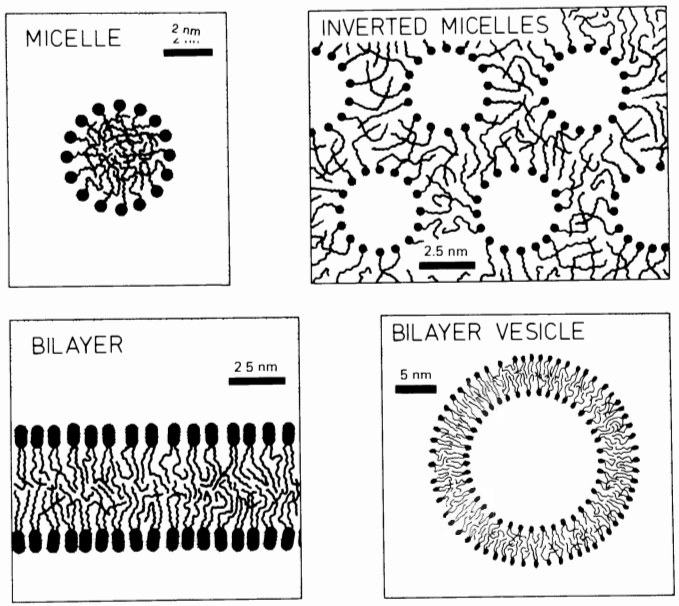

Fig. 16.1. Amphiphiles such as surfactants and lipids (see Table 16.1) can associate into a variety of structures in aqueous solutions. These can transform from one to another by changing the solution conditions such as the electrolyte or lipid concentration, pH, or temperature. In most cases the hydrocarbon chains are in the fluid state allowing for the passage of water and ions through the narrow hydrophobic regions, e.g., across bilayers. The lifetime of water molecules in lecithin vesicles is about 0.02 s, while ions can be trapped for much longer times, about 8 h for Cl^- and one month for Na^+ ions. Most single-chained surfactants form micelles, while most double-chained surfactants form bilayers, for reasons that are discussed in Chapter 17.

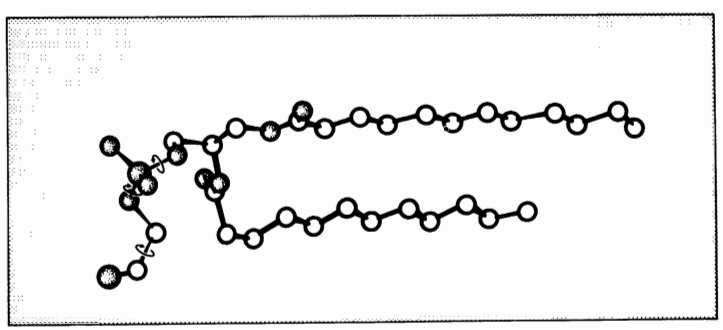

Fig. 16.2. The zwitterionic phospholipid dilauryl-phosphatidyl-ethanolamine containing two saturated hydrocarbon chains and a polar (hydrophilic) headgroup (see also Table 16.1).

different amphiphiles will assemble. We shall find that a very beautiful picture emerges that brings out the role of molecular geometry in determining the structures formed, and from which many of the physical properties of these structures can be quantitatively understood without requiring a detailed knowledge of the very complex short-range forces operating between the polar headgroups and hydrocarbon chains. (By analogy, the van der Waals equation of state contains no information on the nature and range of intermolecular forces, i.e., the force laws, and yet provides a very satisfactory description of gas–liquid phase behaviour. Indeed, when van der Waals in 1873 proposed his famous equation he knew nothing about the origin and nature of van der Waals forces.)

16.2 FUNDAMENTAL THERMODYNAMIC EQUATIONS OF SELF-ASSEMBLY

The literature on this subject is voluminous and often confusing, the most rigorous treatment being that of Hall and Pethica (1967) based on Hill's classic book on small systems thermodynamics (Hill, 1963, 1964). We shall follow the more simplified approach and notation of Tanford (1973, 1980) for micelles, which was later extended to larger lipid aggregates such as bilayers, vesicles, other micellar phases and microemulsion droplets by Nagarajan and Ruckenstein (1977, 1979), Israelachvili *et al.* (1976, 1977, 1980a), Wennerström and Lindman (1979), Mitchell and Ninham (1981), Szleifer *et al.* (1985, 1986), Blanckstein *et al.* (1986), Israelachvili (1987c), and Puvvada and Blanckstein (1990).

Equilibrium thermodynamics requires that in a system of molecules that form aggregated structures in solution (Fig. 16.3) the chemical potential of all identical molecules in different aggregates be the same. This may be expressed as

$$\mu = \mu_1^0 + kT \log X_1 = \mu_2^0 + \tfrac{1}{2}kT \log \tfrac{1}{2}X_2 = \mu_3^0 + \tfrac{1}{3}kT \log \tfrac{1}{3}X_3 = \ldots$$

monomers dimers trimers

or

$$\mu = \mu_N = \mu_N^0 + \frac{kT}{N} \log\left(\frac{X_N}{N}\right) = \text{constant}, \qquad N = 1, 2, 3, \ldots, \qquad (16.1)$$

where μ_N is the mean chemical potential of a molecule in an aggregate of aggregation number N, μ_N^0 the standard part of the chemical potential (the

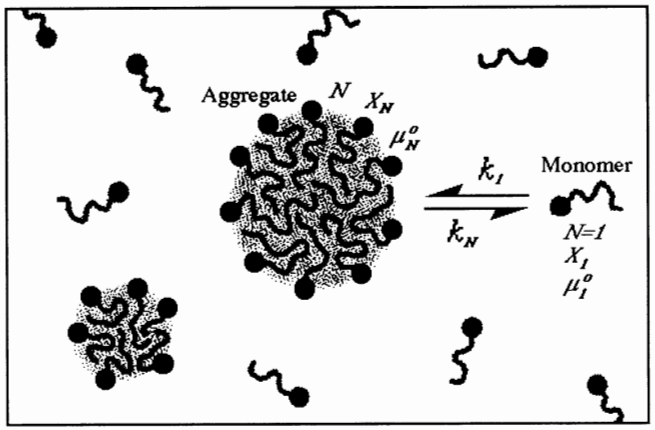

Fig. 16.3. Association of N monomers into an aggregate (e.g., a micelle). The mean lifetime of an amphiphilic molecule in a small micelle is very short, typically 10^{-5}-10^{-3} s.

mean interaction free energy *per molecule*) in aggregates of aggregation number N, and X_N the concentration (more strictly the activity) of molecules in aggregates of number N ($N = 1$, μ_1^0 and X_1 correspond to isolated molecules, or *monomers*, in solution). Equation (16.1) may also be derived using the familiar *law of mass action* (Alexander and Johnson, 1950) as follows: referring to Fig. 16.3 we may write

$$\text{rate of association} = k_1 X_1^N,$$

$$\text{rate of dissociation} = k_N(X_N/N),$$

where

$$K = k_1/k_N = \exp[-N(\mu_N^0 - \mu_1^0)/kT] \tag{16.2}$$

is the ratio of the two 'reaction' rates (the equilibrium constant). These combine to give Eq. (16.1), which can also be written in the more useful (and equivalent) forms

$$X_N = N\{(X_M/M)\exp[M(\mu_M^0 - \mu_N^0)/kT]\}^{N/M} \tag{16.3a}$$

and, putting $M = 1$,

$$X_N = N\{X_1 \exp[(\mu_1^0 - \mu_N^0)/kT]\}^N \tag{16.3b}$$

where M is any arbitrary reference state of aggregates (or monomers) with

aggregation number M (or 1). Equations (16.3) together with the conservation relation for the total solute concentration C

$$C = X_1 + X_2 + X_3 + \cdots = \sum_{N=1}^{\infty} X_N \tag{16.4}$$

completely defines the system. Depending on how the free energies μ_1^0, μ_N^0 are defined the dimensionless concentrations C and X_N can be expressed in volume fraction or mole fraction units ($(\text{mol dm}^{-3})/55.5$ or $M/55.5$ for aqueous solutions). In particular, note that C and X_N can never exceed unity. Equation (16.2) assumes ideal mixing and is restricted to dilute systems where interaggregate interactions can be ignored. The effects of such interactions will be considered later.

□

● WORKED EXAMPLE ●

Question: Certain types of solute molecules are found to self-assemble in solution into discrete macromolecular clusters with a fixed aggregation number N per cluster. The equilibrium between monomers (A) and aggregates (B) in the solution may be expressed in the form of a chemical reaction:

$$A + A + A + \ldots = B.$$

Let X_A and X_B be the concentrations of A and B in mole fraction units, let K be the equilibrium constant for the reaction, and let C be the *total* concentration of solute molecules in the solution.

(i) Obtain a relation between K, N, C and X_A, and show that for $K \gg 1$ and $N \gg 1$ the concentration of monomers, X_A, can never exceed $(NK)^{-1/N}$.

(ii) If $K = 10^{80}$ and $N = 20$ calculate the concentration of molecules in monomers (X_A) and in aggregates (NX_B) at $C = 2 \times 10^{-5}$, $C = 1.052 \times 10^{-4}$ and $C = 10^{-1}$. Comment on your findings. (Note that X_N in the notation of Eqs. (16.1)–(16.4) corresponds to NX_B in the present notation.)

Answer:

(i) Combining the two basic equations: $K = X_B/X_A^N$ and $C = X_A + NX_B$, we obtain $K = (C - X_A)/NX_A^N = \text{constant}$, or $X_A = [(C - X_A)/NK]^{1/N}$. Since the maximum possible value of $(C - X_A)$ is 1, we immediately find that X_A can never exceed $(NK)^{-1/N}$. For $K = 10^{80}$ and $N = 20$ this critical concentration is 0.86×10^{-4}.

(ii) Putting $K = 10^{80}$ and $N = 20$ into the above equation gives $X_A = 10^{-4}[(C - X_A)/20]^{1/20}$. Solving this for the given values of C we find:

at $C = 2 \times 10^{-5}$: $X_A = 1.99999998 \times 10^{-5}$ and $NX_B = 2 \times 10^{-13}$,

at $C = 1.052 \times 10^{-4}$: $X_A = NX_B = 0.526 \times 10^{-4}$,

at $C = 10^{-1}$: $X_A = 0.8 \times 10^{-4}$ and $NX_B = 0.9992 \times 10^{-1}$.

Thus for $C \ll 10^{-4}$ we have $X_A \approx C$ (i.e., most of the surfactant molecules remain dispersed as monomers). At $C \approx 10^{-4}$, we have $X_A \approx NX_B$ (i.e., the molecules partition equally between monomers and aggregates), while for $C \gg 10^{-4}$ we have $X_A \approx 10^{-4} \approx$ constant, and $NX_B \approx C$ (i.e., the monomer concentration remains unchanged at $\sim 10^{-4}$ as all the molecules go into aggregates). The critical concentration of $\sim 10^{-4}$, or $(NK)^{-1/N}$, is known as the *critical micelle concentration*, and is discussed further in Section 16.5. □

Little more can be said about aggregated dispersions without specifying the form and magnitude of μ_N^0 as a function of N. This important matter will now be considered, and it is instructive to first proceed with a formal thermodynamic analysis of the equations derived so far.

16.3 CONDITIONS NECESSARY FOR THE FORMATION OF AGGREGATES

Aggregates form only when there is a difference in the cohesive energies between the molecules in the aggregated and the dispersed (monomer) states. If the molecules in different sized aggregates (including monomers) all experience the same interaction with their surroundings, the value of μ_N^0 will remain constant in different aggregates (with different N), and Eq. (16.3) becomes

$$X_N = NX_1^N \quad \text{for} \quad \mu_1^0 = \mu_2^0 = \mu_3^0 = \cdots = \mu_N^0. \tag{16.5}$$

Since $X_1 < 1$, we must have $X_N \ll X_1$ so that most of the molecules will be in the monomer state ($N = 1$). If μ_N^0 increases as N increases, Eq. (16.3) shows that the occurrence of large aggregates becomes even less probable.

The necessary condition for the formation of large stable aggregates is that $\mu_N^0 < \mu_1^0$ for some value of N, for example, when μ_N^0 progressively decreases as N increases or when μ_N^0 has a minimum value at some finite value of N. As we shall see, the exact functional variation of μ_N^0 with N also determines many of the physical properties of aggregates, such as their mean size and polydispersity. Further, since this variation may be a complex one it is clear that a number of structurally different populations may coexist

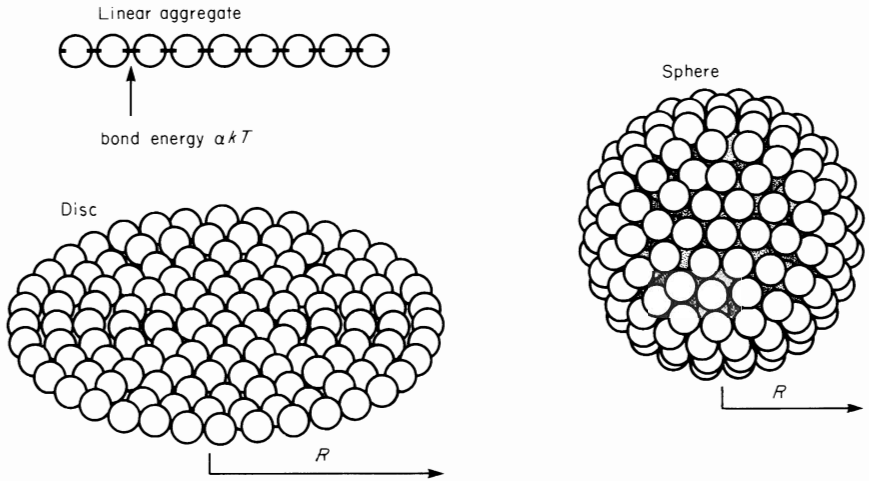

Fig. 16.4. One-, two- and three-dimensional structures formed by the association of identical monomer units in solution.

within a single phase in thermodynamic equilibrium with each other (note that X_N in Eq. (16.3) is a *distribution function* and may peak at more than one value of N).

We shall now consider the functional forms of μ_N^0 for some simple structures and by use of Eqs (16.3)–(16.4) investigate their physical properties.

16.4 VARIATION OF μ_N^0 WITH N FOR SIMPLE STRUCTURES OF DIFFERENT GEOMETRIES: RODS, DISCS AND SPHERES

One-dimensional aggregates (rods)

As mentioned above, aggregates will form if μ_N^0 decreases with N. We shall now see that in a first approximation the dependence of μ_N^0 on N is usually determined by the geometrical shape of the aggregate. Let us begin by considering a suspension of rod-like aggregates made up of linear chains of identical molecules or monomer units (strings of beads) in equilibrium with monomers in solution. Let αkT be the monomer–monomer 'bond' energy in the aggregate relative to isolated monomers in solution (Fig. 16.4). The total interaction free energy $N\mu_N^0$ of an aggregate of N monomers is therefore (remembering that the terminal monomers are unbonded)

$$N\mu_N^0 = -(N-1)\alpha kT,$$

that is,

$$\mu_N^0 = -(1 - 1/N)\alpha kT = \mu_\infty^0 + \alpha kT/N. \tag{16.6}$$

Thus, as N increases the mean free energy μ_N^0 decreases asymptotically towards μ_∞^0, the 'bulk' energy of a molecule in an infinite aggregate. A similar expression for μ_N^0 is obtained for any type of rod-like structure (e.g., a cylindrical micelle).

Two-dimensional aggregates (discs, sheets)

Let us now look at disc-like or sheet-like aggregates (Fig. 16.4). Here the number N of molecules per disc is proportional to the area πR^2, while the number of unbonded molecules in the rim is proportional to the circumference $2\pi R$, and hence to $N^{1/2}$. The mean free energy per molecule in such an aggregate is therefore

$$\mu_N^0 = \mu_\infty^0 + \alpha kT/N^{1/2} \tag{16.7}$$

where again α is some constant characteristic of the monomer–monomer and monomer–solvent interaction.

Three-dimensional aggregates (spheres)

Finally, let us consider spherical aggregates or small solute droplets of radius R in a solvent (Fig. 16.4). Here N is proportional to the volume $\frac{4}{3}\pi R^3$, while the number of unbonded surface molecules is proportional to the area $4\pi R^2$ and hence to $N^{2/3}$. We therefore have

$$\mu_N^0 = \mu_\infty^0 + \alpha kT/N^{1/3}. \tag{16.8}$$

As an example, consider the association of small hydrocarbon molecules such as alkanes in water. If v is the volume per molecule, then $N = 4\pi R^3/3v$. The free energy of the sphere is given by $N\mu_\infty^0 + 4\pi R^2\gamma$, where μ_∞^0 is the bulk energy per molecule and γ the interfacial free energy per unit area (Chapter 15). Hence

$$\mu_N^0 = \mu_\infty^0 + \frac{4\pi R^2\gamma}{N} = \mu_\infty^0 + \frac{4\pi\gamma(3v/4\pi)^{2/3}}{N^{1/3}} = \mu_\infty^0 + \frac{\alpha kT}{N^{1/3}}, \tag{16.9}$$

where

$$\alpha = \frac{4\pi\gamma(3v/4\pi)^{2/3}}{kT} = \frac{4\pi r^2\gamma}{kT}, \tag{16.10}$$

r being the effective radius of a molecule.

We see, therefore, that for the simplest shaped structures—rods, sheets, and spheres—the interaction free energy of the molecules can be expressed as

$$\mu_N^0 = \mu_\infty^0 + \frac{\alpha kT}{N^p}, \tag{16.11}$$

where α is a positive constant dependent on the strength of the intermolecular interactions and p is a number that depends on the shape or *dimensionality* of the aggregates. As we shall see, Eq. (16.11) also applies to various micellar structures and to spherical vesicles in which the bilayers bend elastically. In particular, we note that for all these structures, μ_N^0 decreases progressively with N, which is a necessary condition for aggregate formation.

16.5 THE CRITICAL MICELLE CONCENTRATION (CMC)

Given the general functional form of μ_N^0 of Eq. (16.11) we may now ask, at what concentration will aggregates form? Incorporating Eq. (16.11) into the two fundamental equations of self-assembly, Eqs (16.3) and (16.4), leads to some very interesting conclusions. First, we note that

$$\begin{aligned} X_N &= N\{X_1 \exp[(\mu_1^0 - \mu_N^0)/kT]\}^N \\ &= N\{X_1 \exp[\alpha(1 - 1/N^p)]\}^N \approx N[X_1 e^\alpha]^N. \end{aligned} \tag{16.12}$$

For sufficiently low monomer concentrations X_1 such that $X_1 \exp[(\mu_1^0 - \mu_N^0)/kT]$ or $X_1 e^\alpha$ is much less than unity, we have $X_1 > X_2 > X_3 > \cdots$ for all α. Thus, at low concentrations most of the molecules in the solution will be isolated monomers, i.e., $X_1 \approx C$, as shown in Fig. 16.5. However, since X_N can never exceed unity it is clear from Eq. (16.12) that once X_1 approaches $\exp[-(\mu_1^0 - \mu_N^0)/kT]$ or $e^{-\alpha}$ *it can increase no further.* The monomer concentration $(X_1)_{crit}$ at which this occurs may be called the *critical aggregation concentration* (CAC) though it is common to use the more conventional term *critical micelle concentration* (CMC) to denote the critical

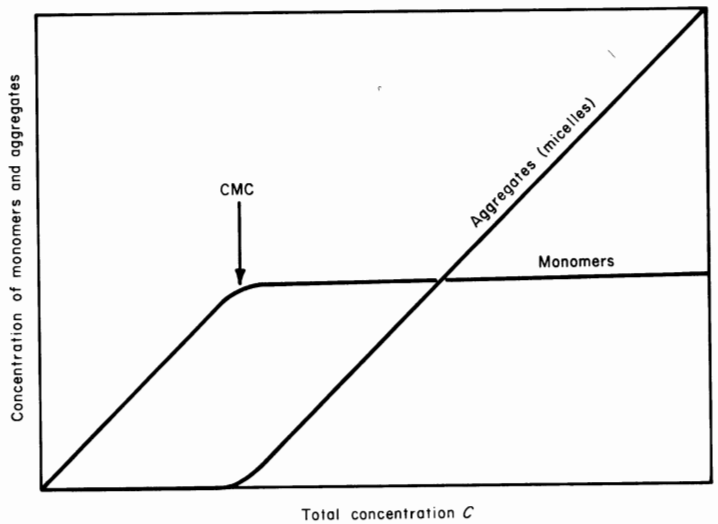

Fig. 16.5. Monomer and aggregate concentrations as a function of total concentration (schematic). Most single-chained surfactants containing 12–16 carbons per chain have their CMC in the range 10^{-2}–10^{-5} M, while the corresponding double-chained surfactants have much lower CMC values due to their greater hydrophobicity. Some important CMC values are listed in Table 16.2.

concentration of all self-assembled structures. Thus, in general

$$(X_1)_{\text{crit}} = \text{CMC} \approx \exp[-(\mu_1^0 - \mu_N^0)/kT]. \qquad (16.13)$$

If μ_N^0 is given by Eq. (16.11), we have

$$(X_1)_{\text{crit}} = \text{CMC} \approx e^{-\alpha} \qquad \text{for all } p. \qquad (16.14)$$

These two equations define the concentration at which further addition of solute molecules results in the formation of more aggregates while leaving the monomer concentration more or less unchanged at the CMC value (Fig. 16.5).

16.6 INFINITE AGGREGATES (PHASE SEPARATION) VERSUS FINITE-SIZED AGGREGATES (MICELLIZATION)

What can we say about the nature of these aggregates? This now depends very much on their shape. For simple disc-like and spherical aggregates,

Eq. (16.12) becomes

$$X_N = N[X_1 e^{\alpha}]^N e^{-\alpha N^{1/2}} \qquad \text{for discs } (p = \tfrac{1}{2}), \qquad (16.15)$$

$$X_N = N[X_1 e^{\alpha}]^N e^{-\alpha N^{2/3}} \qquad \text{for spheres } (p = \tfrac{1}{3}). \qquad (16.16)$$

Above the CMC where $X_1 e^{\alpha} \approx 1$, the above two equations may be approximated by $X_N \approx N e^{-\alpha N^{1/2}}$ and $X_N \approx N e^{-\alpha N^{2/3}}$, respectively. Now for any reasonable positive value of α, which is usually greater than 1, these equations show that apart from a few dimers, trimers, etc., *there will be very few aggregates of any appreciable size* (e.g., with $N > 5$).

Where do the molecules go above the CMC? The answer is quite simple: for discs and spheres, there is a phase transition to a separate phase, strictly to an aggregate of infinite size ($N \to \infty$) at the CMC. Israelachvili *et al.* (1976) showed that such a transition to large macroscopic aggregates occurs whenever $p < 1$ in Eq. (16.11). This applies, quite generally, to all planar or disc-like aggregates composed of identical molecules, and it is for this reason that finite crystalline sheets, one-component lipid bilayers, and even biological membranes with exposed edges are rarely found floating about in solution. Above the CMC infinite bilayers form spontaneously from lipid monomers, although they may close up on themselves to form vesicles (discussed later).

Likewise for simple spherical structures. Here, for example, we may consider the association of oil or alkane molecules in water. On adding oil to water the molecules disperse as monomers up to the critical concentration given by Eqs (16.14) and (16.10),

$$(X_1)_{\text{crit}} \approx e^{-\alpha} \approx e^{-4\pi r^2\gamma/kT}, \qquad (16.17)$$

above which they will separate out into a bulk oil phase, which may be considered simply as a very large spherical aggregate.

For such a system of two immiscible liquids it is clear that what we are now really talking about is the *solubility* of a solute in a solvent, where α represents the free energy of transferring a solute molecule from the solute into the solvent phase. For example, if we consider the solubility of hydrocarbons in water, we may put $\gamma \approx 50\ \text{mJ m}^{-2}$ and $r \approx 0.2$ nm for a methane molecule. Thus, the free energy of transferring a methane molecule from bulk hydrocarbon liquid into water should be approximately $4\pi r^2\gamma \approx 2.5 \times 10^{-20}$ J, corresponding to $\alpha \approx 6$ or about $15\ \text{kJ mol}^{-1}$. Surprisingly, this theoretical estimate agrees well with the experimental value for the solubility or 'hydrophobic energy' of methane (see Worked Example in Section 2.3 and Problem 8.2).

The hydrophobic energy of transferring alkyl chains from water into bulk

hydrocarbon (which determines their solubility) or into micelles (which determines their CMC) can be analysed in a similar fashion. Thus, for an alkane chain of radius $r \approx 0.2$ nm and an interfacial energy with water of $\gamma \approx 50$ mJ m^{-2} as above, the hydrophobic energy per unit length will be $2\pi r\gamma \approx 6 \times 10^{-11}$ J m^{-1}. Now, since the CH_2–CH_2 distance along a chain is $l = 0.126$ nm, this value corresponds to 8×10^{-21} J per CH_2 group added to the chain. Experimentally, one finds an increment of about 6.3×10^{-21} J (equivalent to 900 cal mol^{-1} or 3.8 kJ mol^{-1}) per CH_2 group added to a pure alkane chain at 25°C (Tanford, 1980). This corresponds to an increment in α of $6.3 \times 10^{-21}/kT \approx 1.5$ and thus to a lowering of the solubility of alkanes in water by $e^{-1.5} \approx 0.22$, i.e., by a factor of about four, per added CH_2 group (see first row of Table 16.2).

The above applies only to pure alkane chains being transferred from water into a pure bulk hydrocarbon phase. In the case of surfactant molecules being transferred into micelles or bilayers, the hydrophobic energy increment is significantly lower, ranging from 1.7 to 2.8 kJ mol^{-1} per CH_2 group (Table 16.2). As discussed in Section 8.7 the reduced hydrophobicity of an amphiphilic chain compared to that of a pure alkane chain is believed to be due to the proximity of the hydrophilic headgroup, and to the higher chain ordering of chains within micelles which acts to reduce the energy even more (Aniansson, 1978). The above range of values means that typical micellar CMCs fall by 0.3 to 0.5 (i.e., by a factor between 2 and 3) per CH_2 group added to the surfactant chain.

The important difference between alkanes and amphiphilic molecules is not so much in their solubility or CMC values but in the ability of amphiphiles to assemble into structures in which μ_N^0 reaches a minimum or constant value at some *finite* value of N. It is for this reason that the aggregates formed are not infinite (→ phase separation) but of finite size (→ micellization). The reasons for *why* and *how* amphiphilic molecules do this will be investigated fully in the following chapter.

16.7 SIZE DISTRIBUTIONS OF SELF-ASSEMBLED STRUCTURES

Micelles and vesicles in equilibrium with each other in solution usually have a finite distribution of sizes about some mean value. The distribution may be narrow or broad (polydisperse), and it may be symmetrical or asymmetrical about the mean. Here we shall investigate how polydispersity comes about, starting with a consideration of aggregates for which $p = 1$ in Eq. (16.11).

TABLE 16.2 CMCs of some common surfactants and lipids showing the effects of chain length, number of chains,[a] type of headgroup, counterion, coion, salt and temperature (see Problem 16.1)

Surfactant ($R_n = C_nH_{2n+1}$)	Total number carbon atoms in chains	CMC[b] (mM)	Increment of CMC per CH_2 group (f)	Average energy per CH_2 group ($\Delta G = RT \ln f$)
Pure *n*-alkanes (no headgroup)	4–8	(solubility)	4.4	3.7 kJ mol^{-1} (880 cal mol^{-1})
Cationic				
Alkyl trimethylammonium bromides				
R_{10}-$N(CH_3)_3^+$ Br^-	10	66	2.1	1.8 kJ mol^{-1}
R_{12}-$N(CH_3)_3^+$ Br^-	12	15	2.1	(430 cal mol^{-1})
R_{14}-$N(CH_3)_3^+$ Br^-	14	3.5	2.0	
R_{16}-$N(CH_3)_3^+$ Br^- (CTAB or HTAB)	16	0.9		
Alkyl trimethylammonium chlorides				
R_{10}-$N(CH_3)_3^+$ Cl^-	10	63	1.8	1.7 kJ mol^{-1}
R_{12}-$N(CH_3)_3^+$ Cl^-	12	19	2.1	(400 cal mol^{-1})
R_{14}-$N(CH_3)_3^+$ Cl^-	14	4.5	1.9	
R_{16}-$N(CH_3)_3^+$ Cl^-	16	1.3	2.0	
R_{18}-$N(CH_3)_3^+$ Cl^-	18	0.34		
Anionic				
Sodium alkyl sulphates				
R_8-SO_4^- Na^+	8	130.	2.0	1.7 kJ mol^{-1}
R_{10}-SO_4^- Na^+	10	33.2	2.0	(410 cal mol^{-1})
R_{12}-SO_4^- Na^+ (SDS)	12	8.1	2.0	
R_{14}-SO_4^- Na^+	14	2.0		

TABLE 16.2 (contd) CMCs of some common surfactants and lipids showing the effects of chain length, number of chains,[a] type of headgroup, counterion, coion, salt and temperature (see Problem 16.1)

Non-ionic				
Alkyl polyoxyethylene monoethers				
R_8-$(OCH_2CH_2)_6OH$ (C_8E_6)	8	9.8	3.3	2.9 kJ mol^{-1}
R_{10}-$(OCH_2CH_2)_6OH$ ($C_{10}E_6$)	10	0.90	3.2	(700 cal mol^{-1})
R_{12}-$(OCH_2CH_2)_6OH$ ($C_{12}E_6$)	12	0.087		
Zwitterionic				
Lyso-phosphatidylcholines at 25°C				
R_{10}-PC	10	7.0	3.2	2.8 kJ mol^{-1}
R_{12}-PC	12	0.70	3.2	(680 cal mol^{-1})
R_{14}-PC	14	0.070	3.2	
R_{16}-PC	16	0.007		
Effect of salt				
Sodium alkyl sulphates in 0.3 M NaCl at	8	67	3.1	2.8 kJ mol^{-1}
21°C (note the lower CMCs and higher	10	6.9	3.1	(670 cal mol^{-1})
increment factors than in salt-free water)	12	0.7		
Counterion effects				
Dodecyl sulphate (40°C) in 0.02 M of				
Cs_2SO_4	12	3.0		
K_2SO_4	12	3.5		
Na_2SO_4	12	3.8		
Li_2SO_4	12	4.0		
Co-ion effects				
Dodecyl sulphate (21°C) in 0.1 M of				
NaF	12	1.45		
NaCl	12	1.45		
NaBr	12	1.43		
NaI	12	1.38		
Temperature effects				
Sodium dodecyl sulphate (SDS)	10°C	8.7		
	15°C	8.4		
	20°C	8.3		
	25°C	8.1 ← min		
	30°C	8.3		
	35°C	8.4		
	40°C	8.7		
Double-chained surfactants				
Di-alkyl dimethylammonium chlorides				
R_8R_8-$N(CH_3)_2^+$ Cl^-	16	27	1.9	1.6 kJ mol^{-1}
$R_{10}R_{10}$-$N(CH_3)_2^+$ Cl^-	20	2.0	1.9	(380 cal mol^{-1})
$R_{12}R_{12}$-$N(CH_3)_2^+$ Cl^-	24	0.15		
Di-alkyl sulphates (40°C)				
R_7R_6-CH-SO_4^- Na^+	14	9.70	1.5	1.2 kJ mol^{-1}
R_7R_7-CH-SO_4^- Na^+	15	6.65	1.6	(300 cal mol^{-1})
R_8R_7-CH-SO_4^- Na^+	16	4.25	1.8	
R_8R_8-CH-SO_4^- Na^+	17	2.35	1.6	
R_9R_9-CH-SO_4^- Na^+	19	0.94		
$R_{14}R_{14}$-$CHSO_4^-$ Na^+	29	0.08		
Di-acyl phosphatidylcholines				
R_6R_6-PC	12	1.5×10^{-2} M	2.7	2.1 kJ mol^{-1}
R_8R_8-PC	16	3×10^{-4} M	2.7	(500 cal mol^{-1})
$R_{10}R_{10}$-PC	20	5×10^{-6} M	2.2	
$R_{16}R_{16}$-PC (DPPC)	32	5×10^{-10} M		

[a] All values refer to saturated chains; unsaturated chains have lower interfacial energies with water and higher solubilities (Table 15.1) and are expected to have much lower CMCs than their saturated counterparts. Note that most biological lipids are unsaturated.

[b] Values in water (no added salt) at 25°C unless stated otherwise. CMC and solubility values taken from Mukerjee and Mysels (1970), Shinoda *et al.* (1963), Tanford (1980), Cevc and Marsh (1987), Stafford *et al.* (1989), and Marsh (1990).

Putting $p = 1$ in Eq. (16.12) we obtain

$$X_N = N[X_1 e^{\alpha}]^N e^{-\alpha}. \tag{16.18}$$

Thus, in contrast to Eqs (16.15) and (16.16) the second exponential term is now a constant rather than a rapidly decreasing function of N. Since above the CMC we have $X_1 e^{\alpha} \leqslant 1$, this equation shows that $X_N \propto N$ for small N, i.e., the concentration of molecules in these aggregates now *grows* in proportion to their size, and there is no phase separation. Only for very large N does the $[X_1 e^{\alpha}]^N$ term begin to dominate, eventually bringing X_N down to zero as N approaches infinity. The distribution is therefore highly polydisperse.

The case of $p = 1$ is in marked contrast to the case when $p < 1$ (as occurs for simple discs or spheres) where an abrupt phase transition to one infinitely sized aggregate occurs at the CMC and where the concept of a size distribution does not arise. Alternatively, for structures where $p > 1$ it can be shown that no finite or infinite sized aggregates form at any concentration so that again the concept of a size distribution does not apply (except for the few very small aggregates or clusters of molecules that are always present). Thus structures for which $p = 1$ appear to have special properties, and it is instructive to analyse this type of system in more detail.

The total concentration of molecules is given by inserting Eq. (16.18) into Eq. (16.4) as

$$\begin{aligned} C &= \sum_{N=1}^{\infty} X_N = \sum_{N=1}^{\infty} N[X_1 e^{\alpha}]^N e^{-\alpha} \\ &= e^{-\alpha}[X_1 e^{\alpha} + 2(X_1 e^{\alpha})^2 + 3(X_1 e^{\alpha})^3 + \cdots] \\ &= X_1/(1 - X_1 e^{\alpha})^2, \end{aligned} \tag{16.19}$$

where we have made use of the identity

$$\sum_{N=1}^{\infty} N x^N = x/(1 - x)^2.$$

Thus,

$$X_1 = \frac{(1 + 2Ce^{\alpha}) - \sqrt{1 + 4Ce^{\alpha}}}{2Ce^{2\alpha}}. \tag{16.20}$$

Note that at low concentrations C where $Ce^{\alpha} \ll 1$ this gives $X_1 \approx C$, whereas

at high concentrations, well above the CMC such that $Ce^{\alpha} \gg 1$, the above simplifies to

$$X_1 \approx (1 - 1/\sqrt{Ce^{\alpha}})e^{-\alpha} \leqslant e^{-\alpha}, \tag{16.21}$$

that is, $X_1 \approx$ CMC as expected. Also above the CMC, the density distribution of *molecules* in aggregates of N molecules is given by inserting the above equation back into Eq. (16.18), yielding

$$X_N = N(1 - 1/\sqrt{Ce^{\alpha}})^N e^{-\alpha} \approx Ne^{-N/\sqrt{Ce^{\alpha}}} \qquad \text{for large } N. \tag{16.22}$$

This function peaks at $\partial X_N/\partial N = 0$, which occurs at

$$N_{\max} = M = \sqrt{Ce^{\alpha}}, \tag{16.23}$$

while the *expectation value* of N, defined by $\langle N \rangle = \Sigma N X_N / \Sigma X_N = \Sigma N X_N / C$, is given by

$$\begin{aligned} \langle N \rangle &= \sqrt{1 + 4Ce^{\alpha}} \\ &\approx 1 \qquad \text{below the CMC,} \\ &\approx 2\sqrt{Ce^{\alpha}} = 2M \qquad \text{above the CMC.} \end{aligned} \tag{16.24}$$

Finally, from Eq. (16.22) the density distribution of *aggregates* above the CMC is

$$X_N/N = \text{Const.}\, e^{-N/M} \qquad \text{for } N > M \tag{16.25}$$

i.e., the concentration of large aggregates decays exponentially with increasing N with a characteristic decay number of M. Thus, the distribution is very broad, with the concentration of aggregates first increasing with N for small aggregates and decaying gradually to zero at large N.

The above results should apply to all dilute *one-component* aggregates for which $p = 1$ in Eq. (16.11). This includes any chain-like (polymer-like) aggregates, cylindrical micelles and fibrous structures such as microfilaments and microtubules. Later, we shall see that it also applies to spherical vesicles and microemulsion droplets whose membranes bend elastically. For all these structures, the mean aggregation number M is concentration dependent, varying with the square root of the concentration C above the CMC, and from Eq. (16.23) we note that it is also very sensitive to small changes in the interaction parameter α. Consequently, we may anticipate that the aggregation

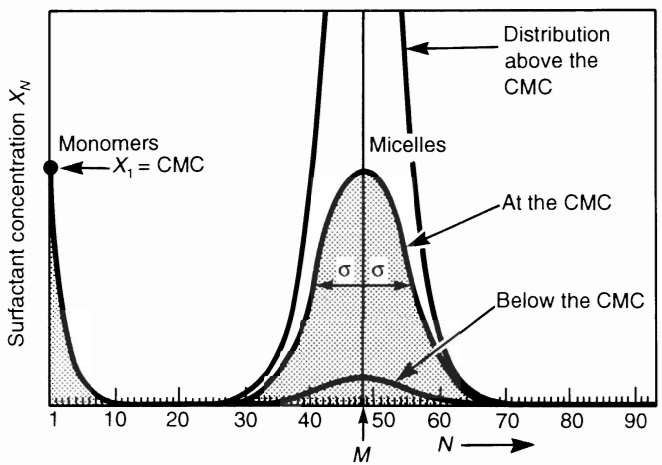

Fig. 16.6. Distribution of molecules X_N as a function of aggregation number N. Near the CMC (shaded region) we have $X_1 \approx X_M$ where the mean micellar aggregation number is M. For spherical micelles, the distribution about M is near Gaussian with standard deviation $\sigma \approx \sqrt{M}$ (see Section 17.4).

number and polydispersity of such structures in water should also be very sensitive to temperature, electrolyte concentration and pH.

Actually, there is a formal relationship between the mean aggregation number, M, the total surfactant concentration, C, and the polydispersity, σ (Fig. 16.6). This relation

$$\sigma^2 \approx \partial \log \langle N \rangle / \partial \log C \tag{16.26}$$

is valid above the CMC (Israelachvili *et al.*, 1976) and shows that whenever the distribution is highly polydisperse, the mean aggregation number is also very sensitive to the total surfactant concentration. Conversely, monodisperse structures have aggregation numbers that do not vary with concentration.

16.8 MORE COMPLEX AMPHIPHILIC STRUCTURES

The value of p in Eq. (16.11) is constant only for aggregates composed of fairly simple molecules that self-assemble into simple geometric shapes such as spheres, discs or rods. More complex amphiphilic molecules can assemble into more complex shapes such as vesicles, interconnected rods or even three-dimensional 'periodic' structures (cf. Fig. 17.10).

Before proceeding with an analysis of the size distribution of these structures, let us first consider what causes different amphiphilic molecules to aggregate into one or another of these structures in the first place. This is determined by the types of anisotropic binding forces acting between different parts of the amphiphilic molecules. For simple (non-amphiphilic) molecules such as alkanes in water whose hydrophobic interaction with each other is largely isotropic or *non-directional*, we would expect them to coalesce and grow as small spherical droplets (for which the total surface energy is a minimum for any given N). And we have seen that for such aggregates, $p = \frac{1}{3}$ in Eq. (16.11), which results in a phase separation at the solubility limit (the effective CMC). Clearly, molecules that aggregate into linear or sheet-like structures must have asymmetric *directional* bonding. For example, cigar-shaped molecules may have their binding sites located at the ends of the molecules or axially around each molecule; the former will result in linear rod-like aggregates, the latter in sheet-like aggregates.

Further, if the molecules are also flexible, the structures they adopt will be more varied than any of the simple shapes so far considered. Thus, the energetically unfavourable regions at each end of a rod-like aggregate may be eliminated if the two ends bend and join together, resulting in a torus or 'toroidal micelle'. Similarly, the unfavourable rim energy of a disc may be eliminated by its closing up into a vesicle, which is what happens with certain classes of surfactants and lipids. In all such cases, μ_N^0 no longer decays gradually with increasing N as given by the simple equation, Eq. (16.11). Instead, it now reaches a minimum value at some *finite* value of N (say $N = M$), or it reaches a low value at $N = M$ and then remains almost constant for $N > M$ (see Fig. 17.5). Depending on the sharpness of the minimum, such a form for μ_N^0 generally results in monodisperse aggregates of mean aggregation number $N < M$, rather than infinite or polydisperse aggregates. As we shall see in the following chapter, this is what happens for certain types of vesicles and spherical micelles. Here we shall consider the consequences for the size distribution of micelles when μ_N^0 reaches a low value at some finite aggregation number M and does not continue to decrease for $N > M$.

To a high degree of accuracy the CMC may be expressed as

$$\text{CMC} \approx \exp[-(\mu_1^0 - \mu_M^0)/kT]. \tag{16.27}$$

This is the common form of the equation traditionally used in the analysis of spherical micelles. If μ_N^0 has a minimum value at $N = M$, the variation of μ_N^0 about μ_M^0 can usually be expressed in the parabolic form:

$$\mu_N^0 - \mu_M^0 = \Lambda(\Delta N)^2 \tag{16.28}$$

where $\Delta N = (N - M)$. In this case Eq. (16.3a) becomes

$$X_N = N\left\{\frac{X_M}{M}\exp[-M\Lambda(\Delta N)^2 kT]\right\}^{N/M} \tag{16.29}$$

and so the distribution of X_N about M will be near Gaussian (Fig. 16.6) with a standard deviation in the *aggregation number* given by

$$\sigma = \sqrt{kT/2M\Lambda}. \tag{16.30}$$

Systems that fall into this category are spherical micelles and certain single bilayer vesicles, and we shall find that for typical values of M and Λ these can be fairly monodisperse with $\sigma/M \approx 0.1$–0.3.

16.9 EFFECTS OF INTERACTIONS BETWEEN AGGREGATES: MESOPHASES AND MULTILAYERS

So far we have ignored interaggregate interactions. These cannot be ignored at high concentrations (low water content) where, especially for surfactant and lipid dispersions, transitions to larger and more ordered *mesophase*[1] or *lyotropic liquid crystalline* structures are commonly observed. These can be ordered arrays of cylinders (*hexagonal* or *nematic* phases), stacks of bilayers (*lamellar*, *liposome* or *smectic* phases) or a complex three-dimensional network of interconnected surfaces (*periodic* structures forming *bicontinuous* phases). Both attractive and repulsive forces between aggregates can lead to such structural phase transitions, and it is worth considering each of these very different scenarios in turn.

First, consider the case where there are strong *repulsive* electrostatic, steric or hydration forces between the aggregates, which we shall assume are initially small spherical micelles. With increasing surfactant concentration the micelles are forced to come closer together, which is energetically unfavourable. However, if the surfactants rearrange to form an ordered array of cylinders, it is a simple matter to ascertain (see Problem 18.5) that their surfaces can now be farther apart from each other. And if they order into a stack of bilayers, their surfaces can be even further apart, all at the same surfactant

[1] A *mesophase* is a normal phase in the thermodynamic sense, but one that is structurally more complex than a simple liquid or solid phase. It can contain many small molecular aggregates that can be monodisperse or polydisperse, or it can have convoluted lamellar or tubular structures that link up with each other to form a repeat three-dimensional network that extends indefinitely throughout the phase. These are known as *periodic* structures, two of which are shown in Fig. 17.10.

concentration (same volume fraction). It is for this reason that many surfactant structures go from being small micelles to long cylinders to large liposomes as the surfactant content is progressively increased above about 10% by weight (Ekwall, 1975; Tiddy, 1980). Note that since these types of phase transitions arise from repulsive forces, where the aggregates are trying to get as far apart as possible within a confined volume of solution, the different phases formed fill up the whole volume of the solution.

When the structural transitions are caused by *attractive* forces the larger structures may now either separate out from, or coexist with, the smaller aggregates or monomers in solution. Such attractive forces arise between uncharged amphiphilic surfaces, e.g., those having nonionic or zwitterionic headgroups, and for charged headgroups in high salt where the electrostatic repulsion is screened. Let us again consider the transformation of small micelles or vesicles into large liposomes. Now, however, because the forces are attractive, the equilibrium separation between the bilayers in the liposomes will be at their potential-energy minimum, where the depth of the minimum is W_0 per unit area (illustrated in Fig. 18.2). While the smaller micelles are clearly favoured entropically, the liposomes could be thermodynamically more favourable if the value of W_0 is sufficiently large. The problem is to establish how these two effects compete in determining which structure is formed at the CMC and at higher concentrations.

If M is the micelle or vesicle aggregation number and $\mathbf{M}$ the liposome aggregation number ($\mathbf{M} \gg M$), then equating the chemical potentials of molecules in all the possible dispersed and aggregated states gives at equilibrium

$$\underset{\text{monomers}}{\mu_1^0 + kT\log X_1} = \underset{\text{micelles/vesicles}}{\mu_M^0 + (kT/M)\log(X_M/M)} = \underset{\text{liposomes/superaggregates}}{\mu_{\mathbf{M}}^0 + (kT/\mathbf{M})\log(X_{\mathbf{M}}/\mathbf{M})} \tag{16.31}$$

$$X_{\mathbf{M}}/\mathbf{M} = \{(X_M/M)\exp[M(\mu_M^0 - \mu_{\mathbf{M}}^0)/kT]\}^{\mathbf{M}/M}. \tag{16.32}$$

The concentration at which $X_{\mathbf{M}} = X_M$ is therefore

$$(X_M)_{\text{crit}} \approx M\exp[-M(\mu_M^0 - \mu_{\mathbf{M}}^0)/kT]. \tag{16.33}$$

Thus, depending on M and the difference in the energies $(\mu_M^0 - \mu_{\mathbf{M}}^0)$ per surfactant molecule in the micellar and liposome states (which includes contributions from both *intra*bilayer and *inter*bilayer interactions) the latter may form spontaneously at the CMC, or—if $(X_M)_{\text{crit}}$ is greater than the CMC—at some higher concentration, while the background concentration

of monomers and the smaller aggregates remains unchanged. We may conveniently term such transitions first and second CMCs. If $\mathbf{M} \gg M$, the concentration at which large aggregates begin to form will be sharp and in all respects analogous to the first CMC. Note, too, that if we put $M = 1$ in Eq. (16.33), it reduces to Eq. (16.13) for the first CMC. Indeed, if we consider the smaller aggregates as if they were 'monomers', Eqs (16.32) and (16.33) are completely analogous to Eqs (16.3) and (16.13).

□

● WORKED EXAMPLE ●

Question: In a certain system the depth of the potential energy minimum between two lipid bilayers is $W = 8 \times 10^{-2}$ mJ m^{-2}. If this is the only energy difference per molecule in a vesicle and in a liposome, estimate the 'critical liposome concentration'. Assume that the surface area occupied by each lipid molecule is 0.70 nm^2, that each vesicle contains 3000 molecules, and that the liposomes are much larger than the vesicles.

Answer: The free energy difference *per molecule* in vesicles and liposomes is

$$(\mu_M^0 - \mu_{\mathbf{M}}^0) \approx \tfrac{1}{2} \times 8 \times 10^{-5} \times 0.70 \times 10^{-18} = 2.8 \times 10^{-23} \text{ J},$$

or 0.0068 kT at 298 K. (*Note*: this corresponds to g_0 in Fig. 18.2.) If $M = 3000$ is the vesicle aggregation number, then from Eq. (16.33) a vesicle-to-liposome transition will occur at a lipid concentration of

$$(X_M)_{\text{crit}} = 3000 \exp(-3000 \times 0.0068) \approx 4 \times 10^{-6},$$

that is, at about 2×10^{-4} M (which may be compared with the first CMC of about 10^{-10} M typical of vesicle-forming lipids). This analysis, however, neglects any possible energy difference arising from the different bilayer curvatures in vesicles and planar bilayers which will also contribute to $(\mu_M^0 - \mu_{\mathbf{M}}^0)$ in Eq. (16.33). Curvature effects are discussed in Section 17.9. □

16.10 CONCLUSION

We have gone as far as is possible with a formal analysis of the statistical thermodynamics of self-assembly, and to proceed further we must now consider the different types of interactions occurring between amphiphilic molecules in aggregates more specifically. In Chapter 17 we shall quantify these interactions and in particular investigate how the geometric shape constraints of surfactant and lipid molecules restrict their assembly into aggregates of different shapes. The important conclusion to be drawn from this chapter is that once the aggregates' shape is known their physical properties are necessarily given by the thermodynamic equations developed in this chapter, for example, a dilute dispersion of (one-component) cylindrical micelles *must* be polydisperse and their size *must* increase with concentration. Therein lies the beauty and power of thermodynamics.

PROBLEMS AND DISCUSSION TOPICS

16.1 In the so-called 'pseudo-phase' approximation of the theory of micelles, it is assumed that only two species exist in the solution: monomers and monodisperse micelles all with the same aggregation number, N. The monomers are at a concentration X_1 and the concentration of monomers in the micelles is X_N (note that the *micellar* concentration is X_N/N). For the case where $(\mu_1^0 - \mu_N^0)/kT = 10$, plot the concentration of surfactant monomers X_1 as a function of total concentration C from $C = 0$ to twice the theoretical CMC for $N = 10$, 50 and 500. For each case find the value of C at which $X_1 = X_N$, and comment on the shapes of the curves and how these values compare with the theoretical CMC as calculated using Eq. (16.13).

16.2 Ionic surfactants in water must be considered as a three-component system (unlike non-ionic surfactants which do not dissociate to give off counterions into solution). An ionic surfactant is fully dissociated in the monomer form but only a fraction f is dissociated in the micellar form. Show that above the CMC the concentration X_1 of monomers will not remain constant as shown in Fig. 16.5, but will fall according to $X_1 \approx \text{constant}/C^f(1-f)^f$.

16.3 Estimate the interfacial tension γ_i of an oil–water interface at 25°C where the aqueous phase contains surfactant micelles and where the interface contains a compact (liquid-condensed) surfactant monolayer. Assume that the total surfactant concentration in the aqueous phase is $C = 10^{-2}$ M (well above the CMC), that the micelles have a mean aggregation number of $M = 100$, and that the headgroup area is $a_0 = 0.40$ nm^2. (*Answer*: $\gamma_i \approx (kT/Ma_0)\ln(M/C) \approx 1$ mJ m^{-2}.)